DOI: https://doi.org/10.37434/tpwj2025.02.03

# STRUCTURE AND PROPERTIES OF WELDED JOINTS OF HEAT-RESISTANT TITANIUM ALLOY OF Ti–Al–Zr–Sn–Mo–Nb–Si SYSTEM PRODUCED BY ELECTRON BEAM WELDING

**S.V. Akhonin[1], V.Yu. Bilous[1], E.L. Vrzhyzhevskyi[1], R.V. Selin[1], I.K. Petrychenko[1], S.L. Schwab[1], S.L. Antonyuk[2]**

[1]E.O. Paton Electric Welding Institute of the NASU
11 Kazymyr Malevych Str., 03150, Kyiv, Ukraine
[2]SC "O.K. Antonov ANTK"
1 Mriya Str., 03062, Kyiv, Ukraine

**ABSTRACT**

Heat-resistant titanium-based pseudo-α-alloys have become widely applied in many sectors of modern industry, which is due to a high level of their specific mechanical properties at higher temperatures. Application of electron beam welding technology is the most rational when manufacturing parts and components from heat-resistant titanium alloys. Its special feature are high rates of cooling of the weld metal and HAZ, which complicates welding of heat-resistant titanium alloy Ti–6.5Al–5.3Zr–2.2Sn–0.6Mo–0.5Nb–0.75Si, where the high silicon content ensures lower ductility characteristics at room temperature. The influence of electron beam welding on the weld metal and HAZ structure, and on the mechanical properties of the heat-resistant titanium alloy Ti–6.5Al–5.3Zr–2.2Sn–0.6Mo–0.5Nb–0.75Si was studied. It was found that application of electron beam welding with local heat treatment at 750 °C leads to reduction of the size of packages with Widmanstatten morphology from 50–100 to 20–50 μm and increase in welded joint strength from 996 to 1041 MPa, which corresponds to base metal strength.

**KEYWORDS:** heat-resistant titanium alloy, microstructure, mechanical properties, electron beam welding, local heat treatment

## INTRODUCTION

Heat-resistant titanium alloys combine high specific values of strength, increased characteristics of fatigue and crack propagation resistance, as well as corrosion resistance [1, 2]. However, establishing the possibility of producing sound welded joints of advanced heat-resistant titanium alloys is an urgent task in view of the growing requirements to engine components being designed [3, 4]. Heat-resistant titanium-based pseudo-α-alloys are considered promising materials in aviation and space engineering, and automotive industry, owing to preservation of the α-structure at elevated temperatures, which is due to maintaining the temperature of polymorphic (α→β)-transformation at the highest possible level. During polymorphic (α→β)-transformation, the hexagonal close packed crystal lattice of the more heat-resistant α-titanium loses its stability and develops into a cubic body-centered modification of the less heat-resistant β-titanium [5, 6]. The highest heat resistance is demonstrated by doped alloys of Ti–Si–X systems due to formation in the cast state of a framework of strengthening phases arising during eutectic crystallization [7]. One of the directions for increasing the titanium alloy heat resistance is creation of in-situ composites based on refractory silicide compounds. In Ti–Al–Si system a continuous series of eutectic compositions forms along the surface of isoconcentration of isoconcentration close to 10 at.% Si, where α-Ti is the matrix, and $Ti_5Si_3$ has the role of strengthening phase [8, 9]. One of such promising alloys is the experimental pseudo-α-alloy Ti–6.5Al–5.3Zr–2.2Sn–0.6Mo–0.5Nb–0.75Si, which can be used to manufacture parts of GTE turbocompressor rotor, as well as of the engine and cooling systems of internal combustion engines (ICE), because their specific weight will be two times less, compared to traditional materials [10, 11].

The great majority of structures from heat-resistant titanium alloys are manufactured using the technologies of electron beam welding (EBW) [12, 13]. EBW features are high quality of welding zone protection from contact with atmospheric gases and welding performance in one pass, as well as the possibility of conducting local heat treatment (LHT) of the welded joint in the vacuum chamber right after welding. The possibility of performing local heating and further heat treatment in the vacuum chamber is an essential advantage of EBW technology [14, 15]. Preheating of the welded joints is a rather effective technological measure which is used in welding high-strength steels to prevent cold cracking [16–18].

**Table 1.** Modes of electron beam welding of heat-resistant titanium alloy Ti–6.5Al–5.3Zr–2.2Sn–0.6Mo–0.5Nb–0.75Si

| Mode | Beam current, mA | Welding speed, mm/s | Preheating temperature, °C | LHT temperature, °C | LHT duration, min |
|---|---|---|---|---|---|
| 1 | 90 | 7 | – | – | – |
| 2 | –»– | –»– | 400 | – | – |
| 3 | –»– | –»– | –»– | 750 | 10 |

EBW features high rates of cooling of the weld metal and HAZ, which results in lower strength of the welded joint of heat-resistant titanium alloys in as-welded condition. In case of performance of welded joints on promising heat-resistant titanium alloy Ti–6.5Al–5.3Zr–2.2Sn–0.6Mo–0.5Nb–0.75Si, EBW is more complicated in connection with the high content of silicon, which is several times higher than silicon solubility in titanium in the weld metal [19]. Influence of the thermal cycle of welding leads to structural changes in the weld metal and HAZ of this alloy resulting in development of a stressed state and in formation of cold cracks, considering the low ductility of silicon-alloyed metal [20, 21].

Thus, it is necessary to study the weldability of new generation heat-resistant titanium alloys and to determine the technological welding modes, which will provide an optimal structure of the weld metal and HAZ, in order to achieve a set of high mechanical properties of the welded joints with the strength not less than 90 % of that of the base material.

The objective of this work is studying the influence of electron beam welding on the structure of weld metal and HAZ, as well as mechanical properties of welded joints of heat-resistant titanium alloy Ti–6.5Al–5.3Zr–2.2Sn–0.6Mo–0.5Nb–0.75Si.

## MATERIALS AND EXPERIMENTAL PROCEDURE

Heat-resistant titanium alloy Ti–6.5Al–5.3Zr–2.2Sn–0.6Mo–0.5Nb–0.75Si is highly sensitive to the thermal cycle of welding. Therefore, it is necessary to study the influence of such technological measures, available for electron beam welding, as preheating and local heat treatment in the vacuum chamber, on the possibility of producing defectfree welded joints.

Electron beam welding was performed in UL-144 machine fitted with ELA 60/60 power unit. Plates made cut out of an ingot of heat-resistant titanium alloy of Ti–6.5Al–5.3Zr–2.2Sn–0.6Mo–0.5Nb–0.75Si system produced by electron beam melting, were used for investigations [22]. Hot-rolled plates from the above-mentioned alloy 10 mm thick were produced in a reversible two-roll rolling mill 500/350 of Skoda Company [23]. Rolling began at the temperature of 1050 °C, the temperature of the end of rolling was not lower than 800 °C. After rolling, the metal was annealed at 900 °C for 1 h.

Chemical composition of experimental alloy Ti–6.5Al–5.3Zr–2.2Sn–0.6Mo–0.5Nb–0.75Si was as follows, wt.%: Ti — base; Al — 6.4–6.8; Zr — 5.1–5.4, Sn — 1.8–2.5; Mo — 0.55–0.75; Nb — 0.5–0.6; Si — 0.74–0.76.

EBW of 10 mm thick samples was performed. Samples of heat-resistant Ti–6.5Al–5.3Zr–2.2Sn–0.6Mo–0.5Nb–0.75Si alloy were assembled without edge preparation or a gap. EBW modes for heat-resistant titanium alloy Ti–6.5Al–5.3Zr–2.2Sn–0.6Mo–0.5Nb–0.75Si are given in Table 1. Figure 1 shows an example of a welded joint of heat-resistant Ti–6.5Al–5.3Zr–2.2Sn–0.6Mo–0.5Nb–0.75Si alloy produced by EBW without application of preheating or LHT.

Power of the electron beam during preheating and LHT was 3 kW, which ensured up to 750 °C temperature in the treatment zone. The width of the treatment zone with preheating and LHT along the weld was 30 mm. The temperature in LHT zone was monitored with thermocouples and recorded using a multichannel potentiometer KSP4. Figure 2, *b* gives an example of the thermal cycle in welding with preheating up to 400 °C, Figure 2, *c* presents the recorded thermal cy-

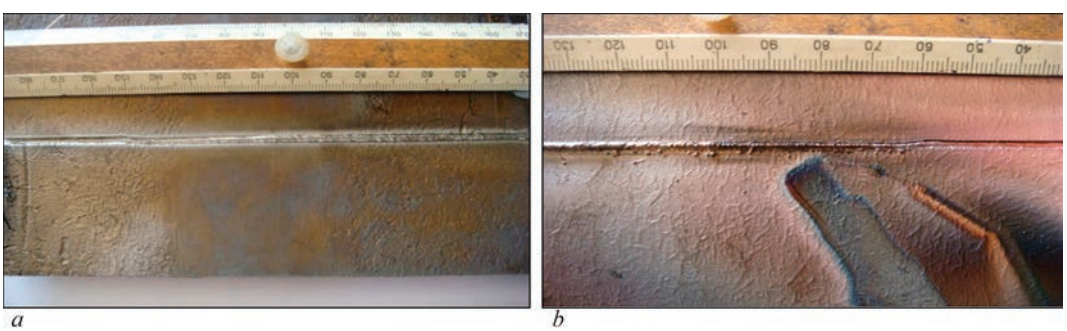

**Figure 1.** Welded joint of heat-resistant titanium alloy Ti–6.5Al–5.3Zr–2.2Sn–0.6Mo–0.5Nb–0.75Si made by EBW (mode 1), in as-welded condition: *a* — face; *b* — root side

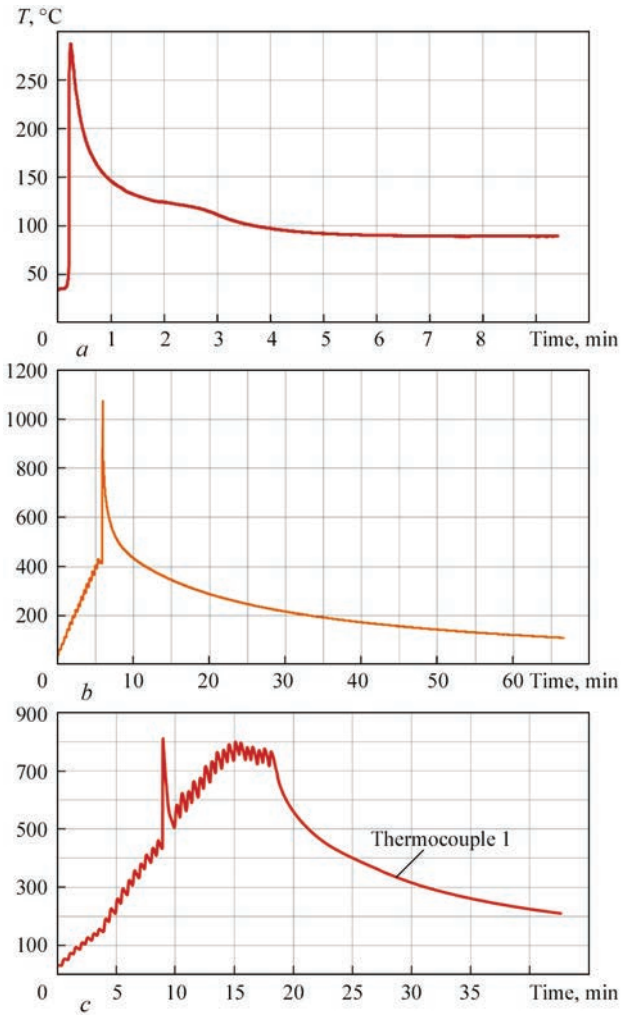


**Figure 2.** Thermal cycle in the HAZ in EBW of heat-resistant Ti–6.5Al–5.3Zr–2.2Sn–0.6Mo–0.5Nb–0.75Si alloy: *a* — without preheating or LHT; *b* — with preheating to 400 °C; *c* — with preheating to 400 °C and further LHT at 750 °C

cle in welding with preheating to 400 °C and postweld LHT at 750 °C.

Examination of transverse sections of EB welded joints on heat-resistant Ti–6.5Al–5.3Zr–2.2Sn–0.6Mo–0.5Nb–0.75Si alloy showed that the macrostructure of the base metal, weld metal and HAZ is more homogeneous in the condition after preheating and LHT (Figure 3).

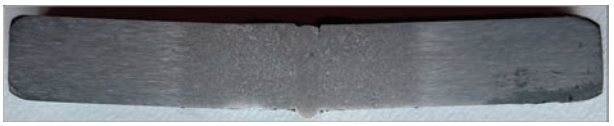

**Figure 3.** Macrosection of as-welded joint of heat-resistant titanium alloy Ti–6.5Al–5.3Zr–2.2Sn–0.6Mo–0.5Nb–0.75Si made by EBW (mode 3)

## MICROSTRUCTURE OF EB WELDED JOINTS OF HEAT-RESISTANT TITANIUM ALLOY Ti–6.5Al–5.3Zr–2.2Sn–0.6Mo–0.5Nb–0.75Si

The Ti–6.5Al–5.3Zr–2.2Sn–0.6Mo–0.5Nb–0.75Si alloy belongs to the group of pseudo-α-alloys, in which the α-phase is the alloy matrix, and a certain amount of the β-phase can form, depending on the specific conditions of microstructure formation. Studies of the initial alloy structure immediately after rolling was over, showed that the metal in as-rolled condition has a fine-grained structure, formed by globular (equiaxed) grains 5–15 μm in size, whereas precipitates of β-phase crystallites are observed along the boundaries of α-phase grains in relatively small amounts (Figure 4).

Before welding, the alloy was vacuum annealed at the temperature of 900 °C. Microstructure analysis indicates that annealing led to a change in the alloy structure morphology (Figure 5, *a*). During cooling after annealing, a Widmanstatten structure (basket weave structure) was formed, which consisted of α- and β-phase platelets. The size of individual packages of the Widmanstatten structure, assessed by the maximal length of the platelets in the package was 20–50 μm (Figure 5, *b*) which is indicative of a significant increase in the size of grains of the matrix α-phase during annealing.

Figure 6 shows the microstructure of weld metal of EB welded joint of heat-resistant Ti–6.5Al–5.3Zr–2.2Sn–0.6Mo–0.5Nb–0.75Si alloy. Image magnification is determined by the scale mark on the respective photo. Microstructure analysis indicates that a typical dendrite structure of cast metal forms in the weld zone (Figure 6, *a*). It is dense and no defects such as porosity, cracks or nonmetallic inclusions are detected in it.

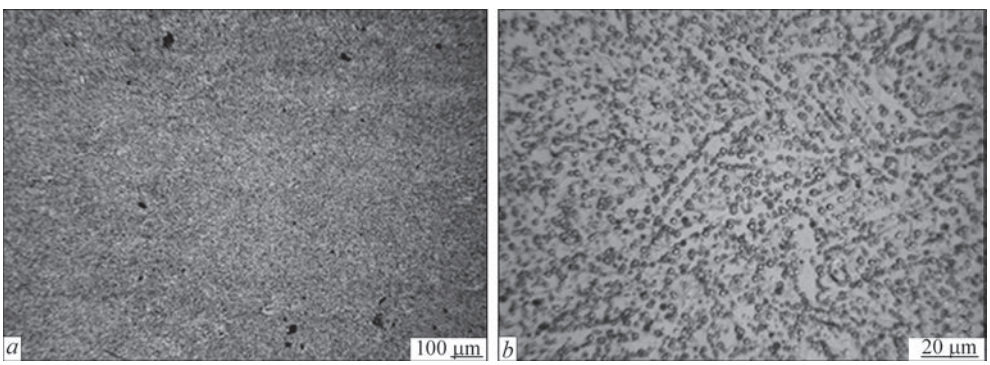


**Figure 4.** Microstructure of the central zone of a hot-rolled sheet of Ti–6.5Al–5.3Zr–2.2Sn–0.6Mo–0.5Nb–0.75Si alloy in as-rolled state

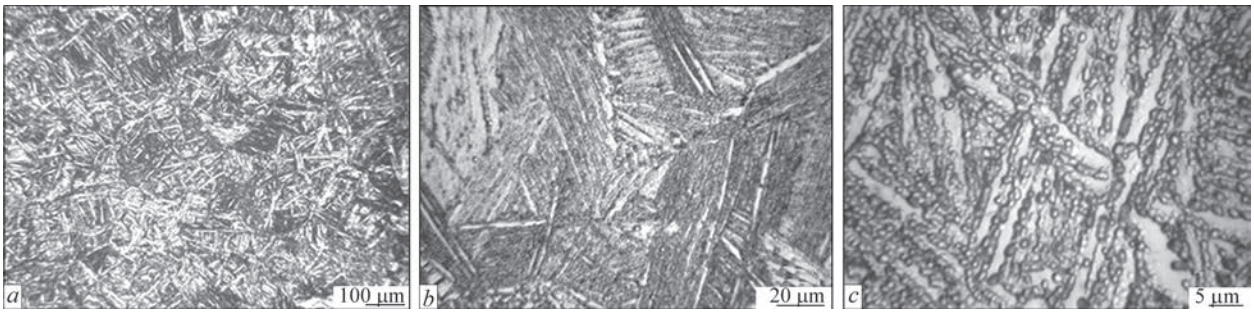


**Figure 5.** Microstructure of the central zone of a 10 mm hot-rolled sheet of Ti–6.5Al–5.3Zr–2.2Sn–0.6Mo–0.5Nb–0.75Si alloy in as-annealed condition

The size of dendrite branches on the section surface can be tentatively assessed by the difference in etchability of individual areas, and it is equal to 100–500 μm. Dendrite area boundaries have no excess phase precipitation, and are not the weak points of the material. It is important that rapid cooling of the molten weld metal in EBW results in formation of rather dispersed packages of Widmanstatten morphology in the dendritic areas with package size (by the size of the largest platelets) in the range of 20–50 μm, which is close to the characteristics of dispersion of base metal structure.

Considering the high rate of cooling to temperatures below $T_{p.tr}$, the intragranular structure of the weld metal is represented by martensite acicular α′-phase (Figure 6, *b*), which forms due to β→α′ transformation. The primary grain boundaries have a thin intermittent α-fringe, the thickness of which is close to 1–2 μm. The martensite needle thickness is 1–2 μm. Dispersed particles of titanium silicides of up to 1 μm size, as well as an intermittent layer between the martensite platelets are also present in the weld metal (Figure 6, *c*).

Microstructure analysis of the HAZ metal of EB welded joint of heat-resistant titanium alloy Ti–6.5Al–5.3Zr–2.2Sn–0.6Mo–0.5Nb–0.75Si indicates that the HAZ metal preserves the main morphological and dimensional characteristics of the base metal (Figure 7).

Obviously, β-phase precipitation in the α-phase matrix, as well as potential formation of $\alpha_2$-phase ($Ti_3Al$) precipitates under the impact of the welding heat and partial decomposition of metastable β-phase blocks the growth of matrix grain. This assumption is further confirmed by a certain reduction of the amount of β-phase observed in the HAZ, compared to the base metal structure. The HAZ width is equal to approximately 500 μm. HAZ metal consists of equiaxed grains with lamellar intragranular structure, the thickness of α-platelets in the colonies being equal to 1.5–5.0 μm (Figure 7, *b*). Dispersed particles from less than 1.0 to 1.5 μm size are localized, mainly, within

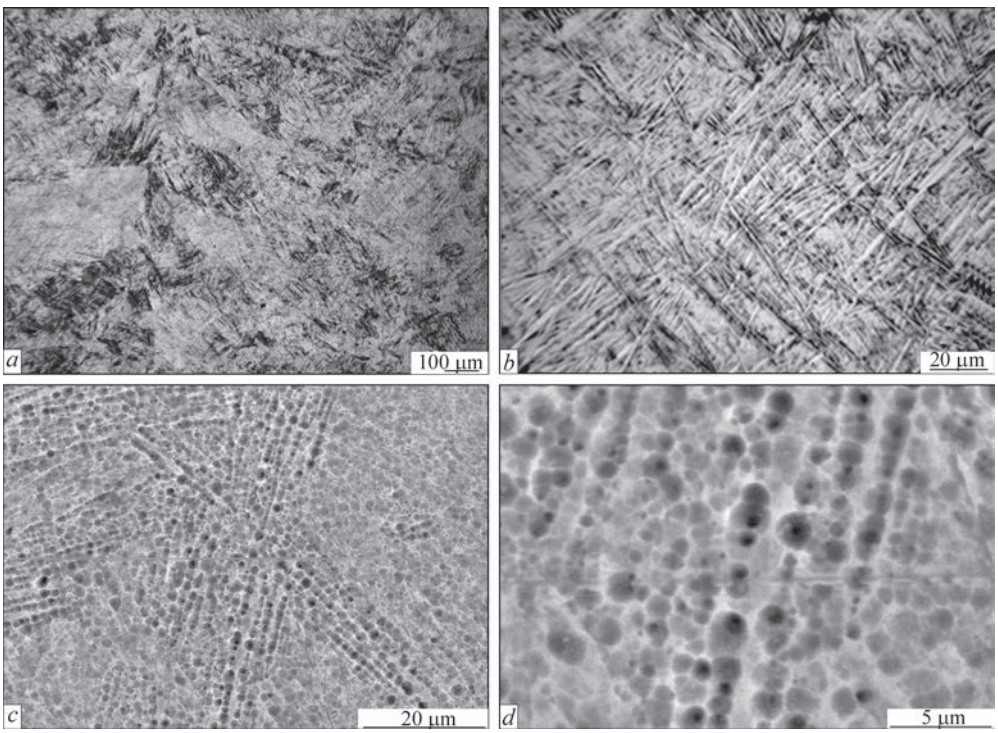


**Figure 6.** Microstructure of weld metal of EB welded joint of heat-resistant Ti–6.5Al–5.3Zr–2.2Sn–0.6Mo–0.5Nb–0.75Si alloy in as-welded condition

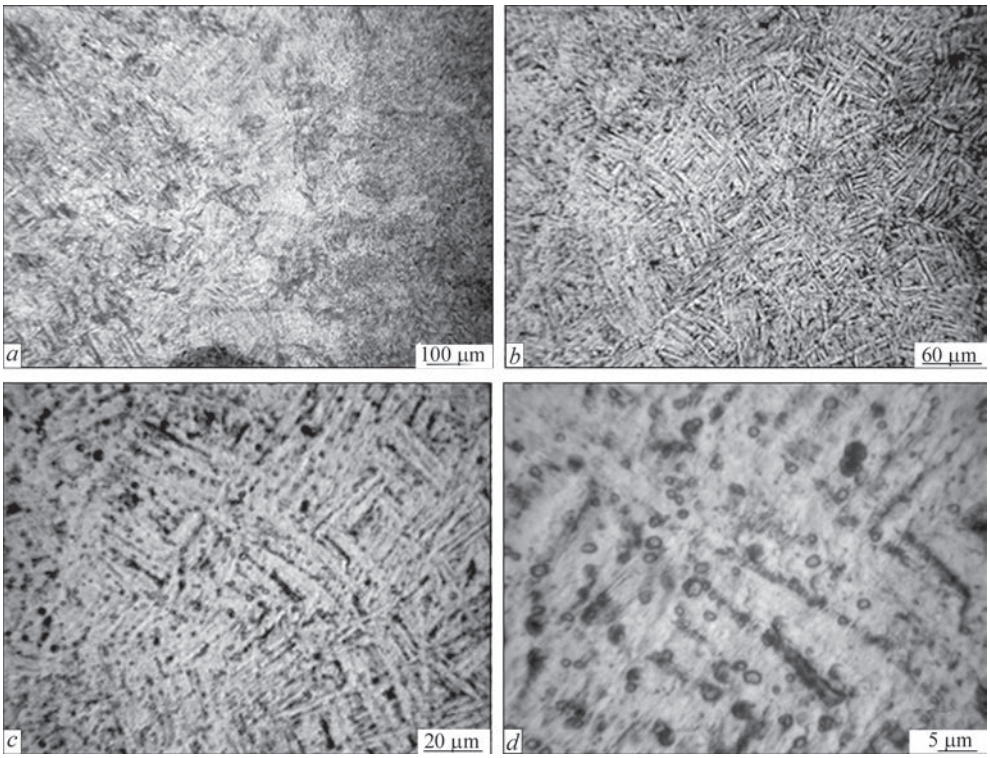


**Figure 7.** Microstructure of HAZ metal of EB welded joint of heat-resistant Ti–6.5Al–5.3Zr–2.2Sn–0.6Mo–0.5Nb–0.75Si alloy in as-welded condition

the platelets. In some places there are elongated layers of another phase between the adjacent platelets of up to 3–8 μm length (Figure 7, *c*, *d*).

Determination of microhardness distribution in EB welded joint of heat-resistant titanium alloy Ti–6.5Al–5.3Zr–2.2Sn–0.6Mo–0.5Nb–0.75Si in as-welded condition led to the conclusion that the microhardness level in different areas of the welded joint is very heterogeneous (Figure 8).

The greatest microhardness values are recorded in the weld metal at the level of 3000 MPa. The lowest level of 2400 MPa was found in the base metal, and the medium one of 2500 MPa was determined in the HAZ metal. It should be noted that a heterogeneous microhardness distribution causes the heterogeneity of the welded joint mechanical properties.

In order to ensure microstructure homogeneity, and homogeneous distribution of microhardness in different areas of welded joints of heat-resistant titanium alloy Ti–6.5Al–5.3Zr–2.2Sn–0.6Mo–0.5Nb–0.75Si, EBW with preheating to 400 °C was used.

Microstructure analysis of weld metal of welded joint of heat-resistant Ti–6.5Al–5.3Zr–2.2Sn–0.6Mo–0.5Nb–0.75Si alloy, made by EBW with preheating to

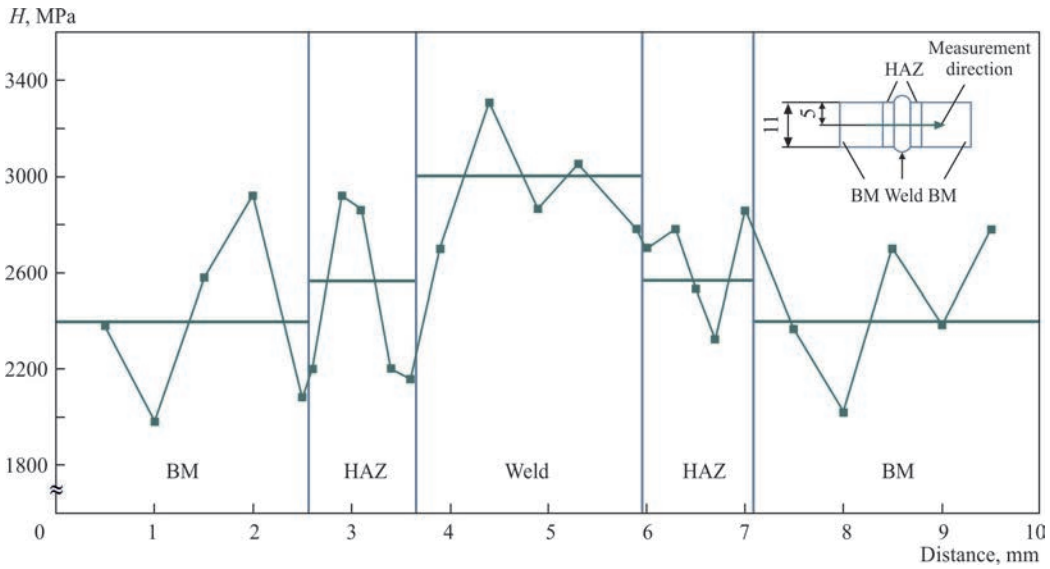


**Figure 8.** Distribution of microhardness (*H*) in EB welded joint of heat-resistant titanium alloy Ti–6.5Al–5.3Zr–2.2Sn–0.6Mo–0.5Nb–0.75Si in as-welded condition

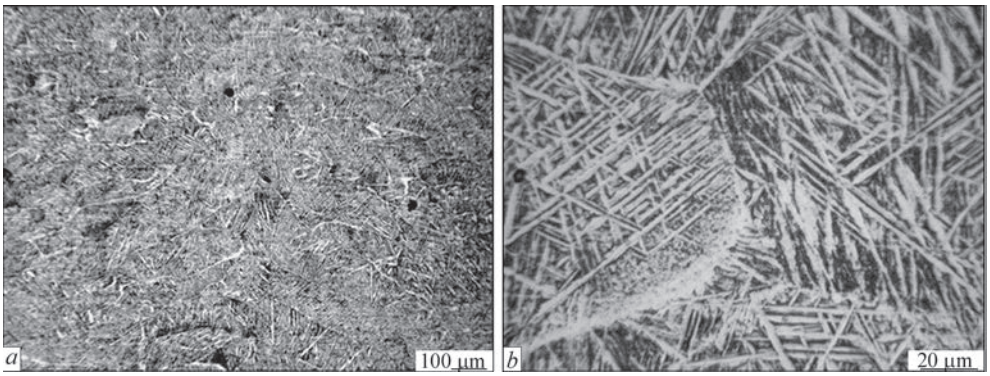


**Figure 9.** Microstructure of weld metal of welded joint of heat-resistant Ti–6.5Al–5.3Zr–2.2Sn–0.6Mo–0.5Nb–0.75Si alloy, made by EBW with preheating to 400 °C, in as-welded condition

400 °C indicates formation of a typical dendrite structure of cast metal in the weld zone (Figure 9). It is dense and no defects such as porosity, cracks or nonmetallic inclusions are indentified in it. The weld metal consists of equiaxed primary β-grains, elongated in the direction of heat removal. The equiaxed grains are localized predominantly along the weld axis.

There is an α-fringe along the primary grain boundaries, the thickness of which is 1.5–7.0 μm (Figure 9, *a*). The size of the dendrite branches in the section plane can be tentatively assessed by precipitation of the α-phase interlayers along the boundaries of the dendrite areas. It is equal to 200–300 μm. Precipitation of such interlayers decreases the structure homogeneity and may potentially facilitate crack propagation during fracture. The intragranular structure consists of martensitic α-phase, which mainly forms small-sized colonies, the colony width being 5–20 μmm (Figure 9, *b*). Platelet thickness is from 1 to 2 μm. Chains of dispersed particles are observed between α-phase platelets.

As in the case of welding without preheating, accelerated cooling of the molten weld metal results in formation of rather dispersed packages of Widmanstatten morphology in the dendritic areas. In this case, however, coarser packages with the size (by the size of the largest platelets) in the range of 50–100 μm are formed that is larger than in welding without preheating, and larger than in the base metal structure. Combined with formation of α-phase interlayers on the boundaries of the dendritic areas and on the boundaries of individual Widmanstatten packages, this can potentially facilitate crack initiation and propagation during destruction.

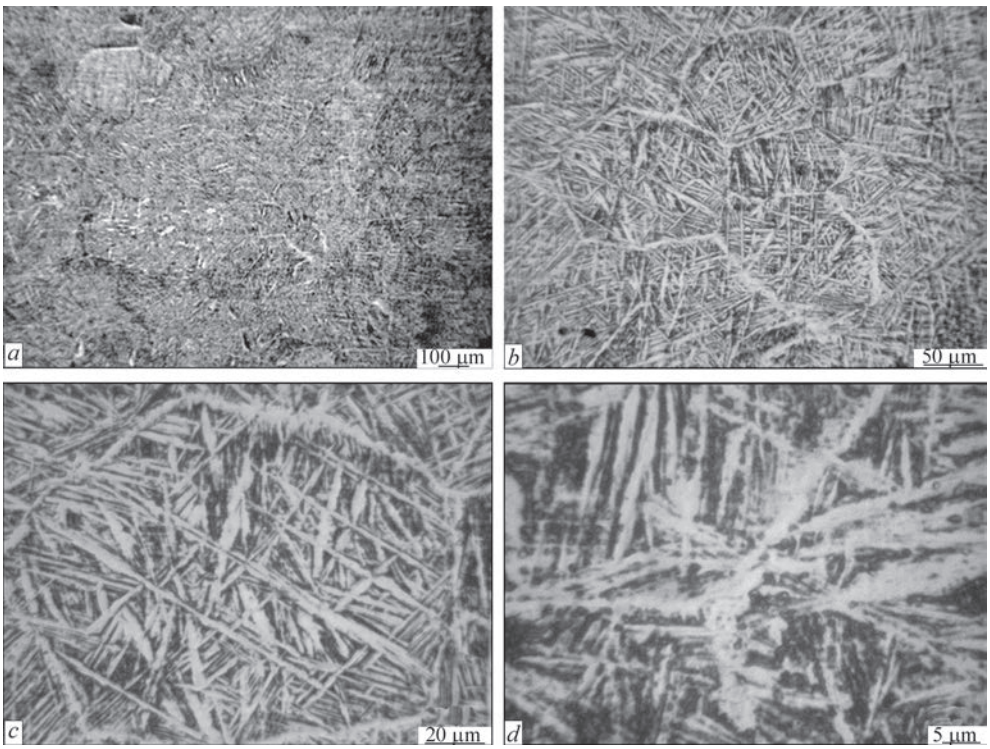


**Figure 10.** Microstructure of HAZ metal of welded joint of heat-resistant Ti–6.5Al–5.3Zr–2.2Sn–0.6Mo–0.5Nb–0.75Si alloy, made by EBW with preheating to 400 °C, in as-welded condition

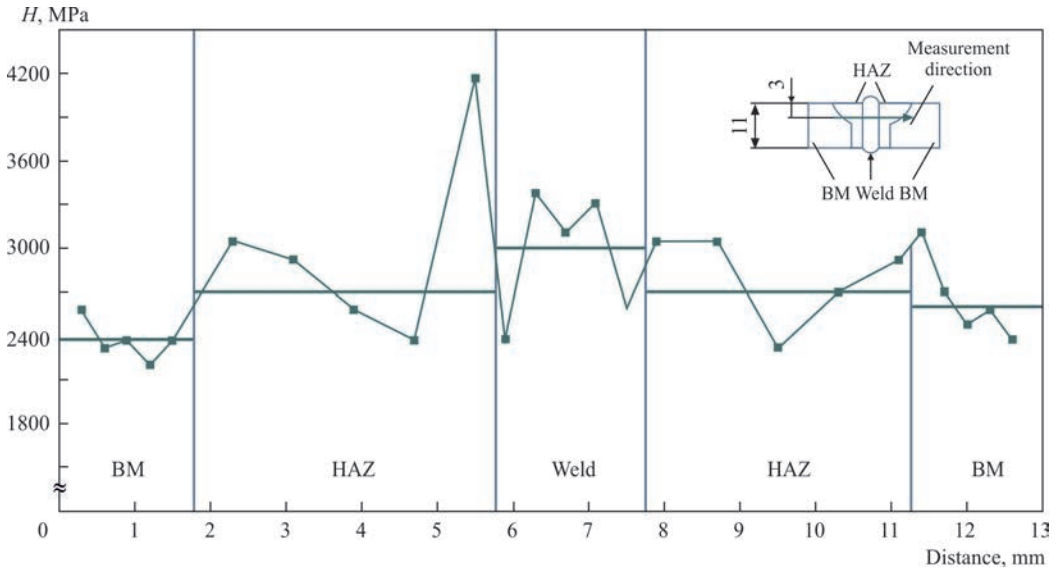


**Figure 11.** Distribution of microhardness (*H*) in welded joint of heat-resistant Ti–6.5Al–5.3Zr–2.2Sn–0.6Mo–0.5Nb–0.75Si alloy made by EBW with preheating to 400 °C, in as-welded condition

Analysis of metal microstructure in the HAZ of the welded joint of heat-resistant titanium alloy Ti–6.5Al–5.3Zr–2.2Sn–0.6Mo–0.5Nb–0.75Si, produced by EBW with preheating to 400 °C, indicates that structure coarsening is observed in the HAZ in welding with preheating, compared to base metal structure (Figure 10). HAZ metal consists of equiaxed primary grains of 50–300 μm size (Figure 10, *b*, *c*) with an α-fringe, the thickness of which is 1–7 μm. The intragranular structure is made up of lamellar α-phase, which forms small colonies of up to 20 μm size (Figure 10, *c*, *d*). Platelet thickness is 1.5–5.0 μm. Isolated dispersed particles and their clusters are observed in the gaps between the platelets (Figure 10, *d*).

Similar phase precipitates were observed also in other areas of the welded joint of this alloy, as well as in the welded joint made by EBW without preheating. It can be noted, that structure of welded joints produced by EBW without preheating and with preheating is identical in the corresponding areas.

Thus, while the main morphological characteristics of base metal (basket weave structure) are preserved, the Widmanstatten package size is somewhat larger, and formation of α-phase interlayers is observed on package boundaries. Additional supply of thermal energy into the welding zone due to preheating in EBW promotes temperature increase in the welding zone and slows down the cooling after completion of the welding process, that leads to significant coarsening of the weld structure and occurrence of grain growth processes in the HAZ.

Establishing the microhardness distribution in EB welded joint of heat-resistant titanium alloy Ti–6.5Al–5.3Zr–2.2Sn–0.6Mo–0.5Nb–0.75Si in the condition after welding with preheating to 400 °C, led to the conclusion that the microhardness level in different areas of the welded joints is also very heterogeneous (Figure 11). The highest microhardness values are recorded in the weld metal at the level of 3000 MPa. The lowest level was found in the base metal at 2400 MPa.

To ensure a uniform distribution of microhardness and a homogeneous microstructure in different areas of welded joints of heat-resistant titanium alloy Ti–6.5Al–5.3Zr–2.2Sn–0.6Mo–0.5Nb–0.75Si, EBW with preheating to 400 °C and LHT at 750 °C for 10 min was used (mode 3, see Table 1).

Analysis of the produced welded joint microstructure (Figure 12) indicates that a typical dendrite structure of cast metal forms in the weld zone. It is dense, and no defects such as porosity, cracks or nonmetallic inclusions were revealed in it. The size of dendrite branches on the section surface is equal to 100–150 μm. The boundaries of the dendritic areas do not contain any excess phase precipitates and are not the material weak points. It is important that rapid cooling of the molten weld metal results in formation in the dendritic areas of rather dispersed packages of Widmanstatten morphology with package size (by the size of the largest platelets) in the range from 20 to 50 μm, which is close to the characteristics of dispersion of the base metal structure.

Smaller primary β-grains of 100–150 μm size (Figure 12, *a*) form in the weld metal than in the case of simple EBW with grains of 300–400 μm size. In addition to equiaxed primary grains localized near the axis, the weld metal also contains non-equiaxed grains, elongated in the direction of the heat removal (Figure 12, ***b)***. The intragranular structure of the weld metal is of lamellar type (Figure 12, *c*), platelet width being 1–2 μm. Dispersed particles 1 μm in size or less are located both along the platelet boundaries, and in the spaces between

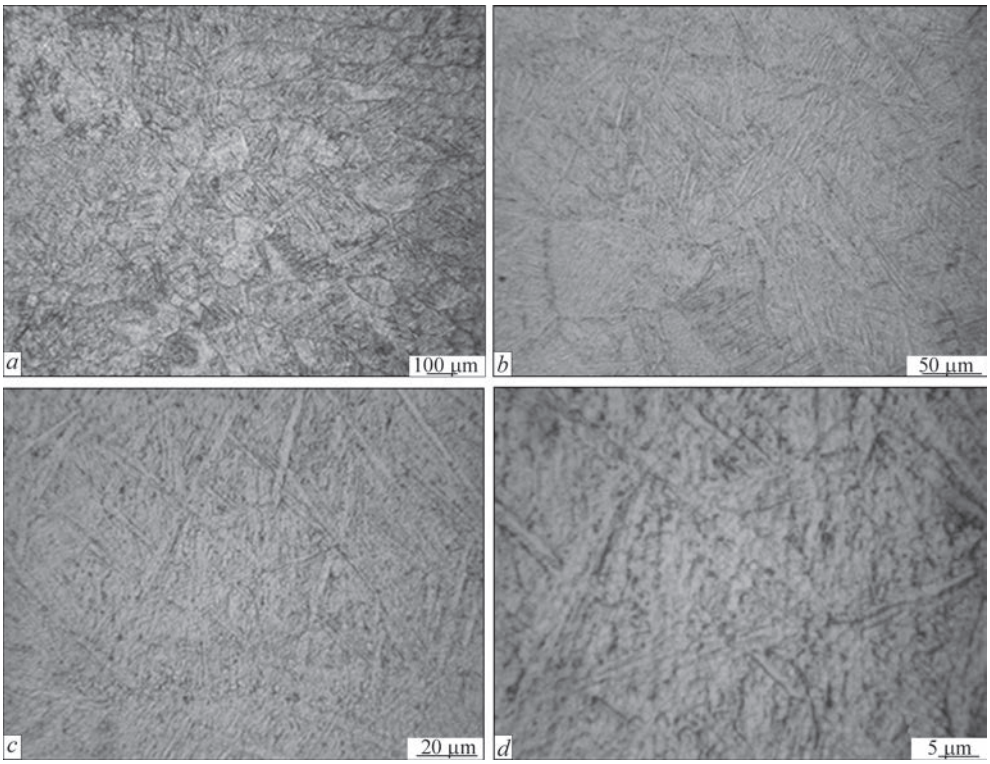


**Figure 12.** Microstructure of weld metal of welded joint of heat-resistant Ti–6.5Al–5.3Zr–2.2Sn–0.6Mo–0.5Nb–0.75Si alloy, made by EBW with LHT at 750 °C

them (Figure 12, *d*). It is obvious that the dispersed particles are titanium silicides ($Ti_5Si_3$), which form in the alloy being welded, due to its increased silicon content, which is higher than its solubility in α-titanium.

The structure of HAZ metal of the samples with different heat treatment is given in Figure 13. Microstructure analysis shows that the HAZ preserves the main morphological and dimensional characteristics of the base metal (Figure 13, *a*).

No differences were observed in the structure after application of different heat treatment modes. A clearer definition of α-phase platelets due to β-phase

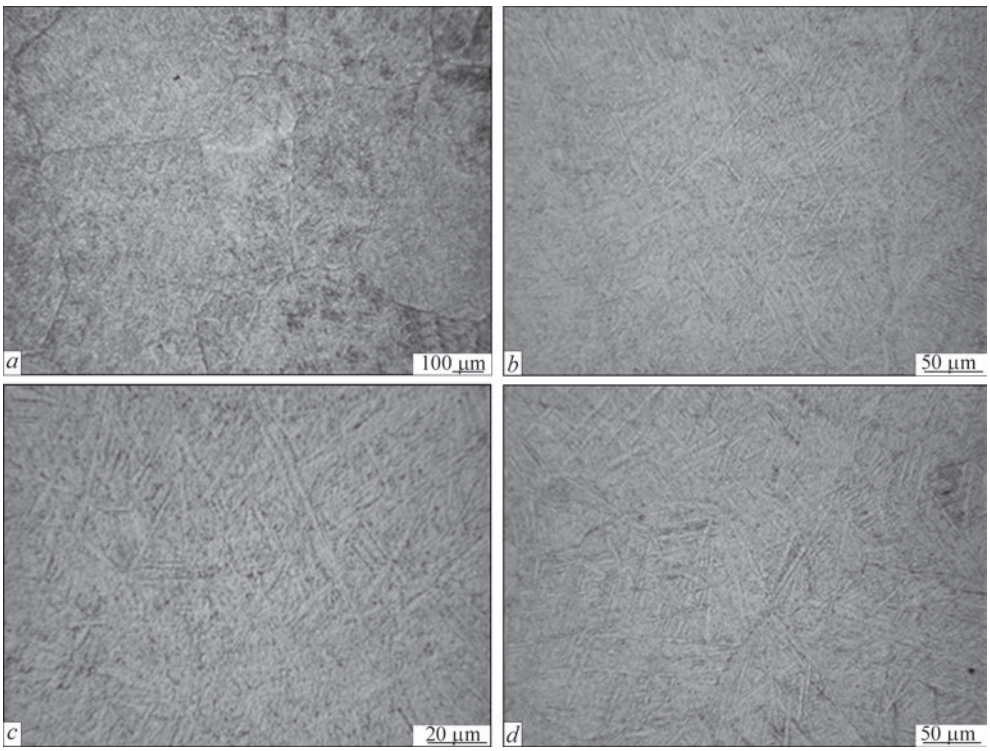


**Figure 13.** Microstructure of HAZ metal of welded joint of heat-resistant Ti–6.5Al–5.3Zr–2.2Sn–0.6Mo–0.5Nb–0.75Si alloy, made by EBW with LHT at 750 °C

precipitation along the platelet boundaries and, possibly, formation of intermetallic particles, is seen in the HAZ structure (Figure 13, *c*). Dispersed particles 1 μm in size and less are located both in the fusion zone near the HAZ along platelet boundaries, and in the spaces between the platelets (Figure 13, *d*). Grain size in the HAZ metal is equal to 200–500 μm.

Although application of different heat treatment modes did not lead to any significant changes in the welded joint microstructure, the difference in the intensity of structure etching and in the amount of β-phase on the boundaries of α-phase platelets suggests that the mechanical properties of the joints could change under the thermal impact, as a result of relaxation of mechanical stresses and formation of excess phases.

Thus, the technology of electron beam welding of heat-resistant Ti–6.5Al–5.3Zr–2.2Sn–0.6Mo–0.5Nb–0.75Si alloy with LHT allows producing a tight joint without porosity, cracks or nonmetallic inclusions. At EBW without heating a relatively fine-grained weld structure forms and there is no HAZ microstructure coarsening.

## DISCUSSION OF THE RESULTS

It should be noted that a considerable coarsening of the weld structure and increase of grain size in the HAZ are observed in EBW with preheating to 400 °C. Therefore, use of just heating for EBW of heat-resistant Ti–6.5Al–5.3Zr–2.2Sn–0.6Mo–0.5Nb–0.75Si alloy is not rational. It can be explained by an undesirable range of cooling rates at EBW with only the preheating. So, the cooling rate in the HAZ in EBW without preheating or LHT is equal to 88–131 °C at 700–800 °C, the cooling rate in the HAZ in EBW with preheating is 30–50 °C/s, and the cooling rate in EBW with preheating to 400 and LHT at 750 °C is 8.3–8.8 °C/s.

Determination of microhardness distribution in the welded joint of heat-resistant titanium alloy Ti–6.5Al–5.3Zr–2.2Sn–0.6Mo–0.5Nb–0.75Si produced by EBW

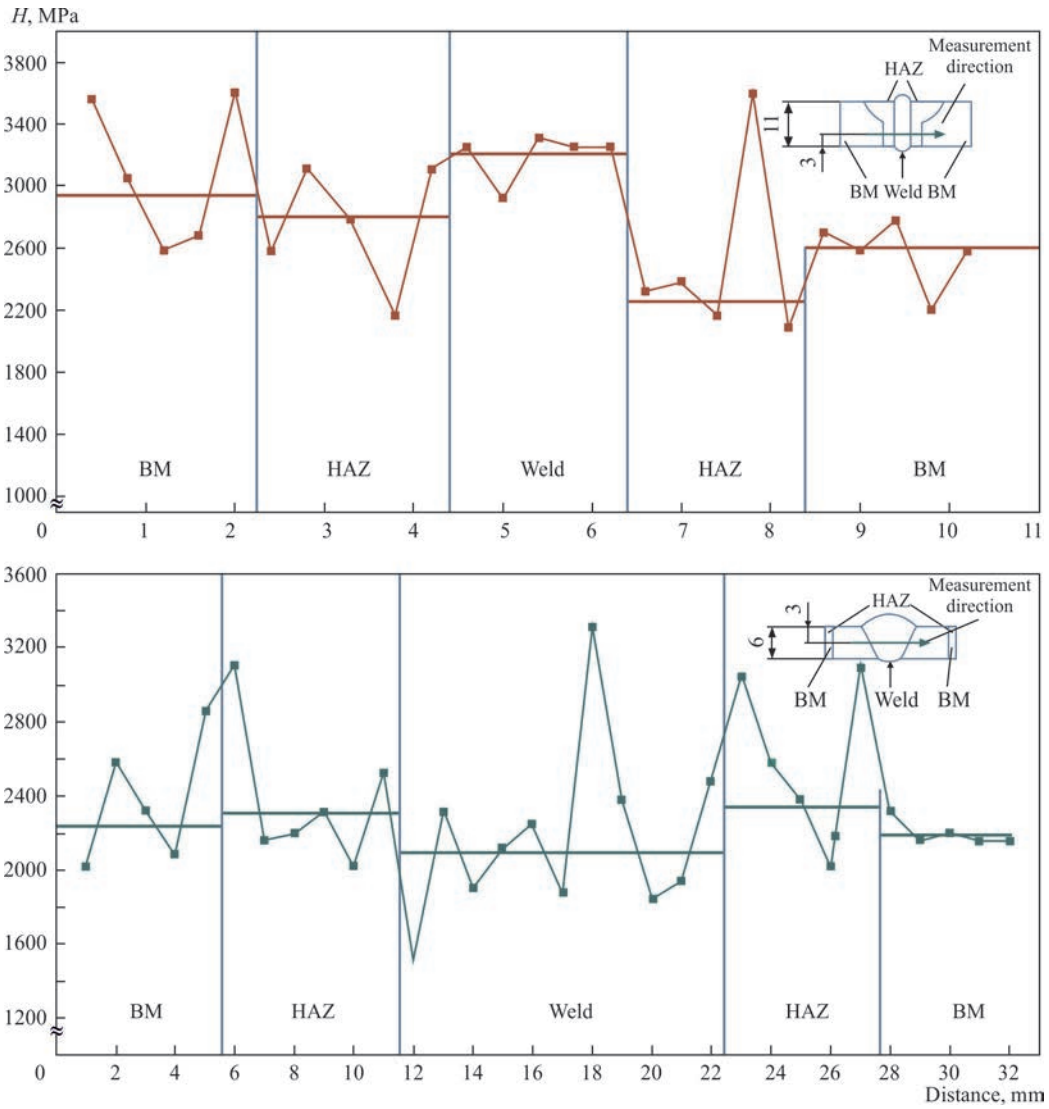


**Figure 14.** Microhardness distribution in EB welded joint of heat-resistant titanium alloy Ti–6.5Al–5.3Zr–2.2Sn–0.6Mo–0.5Nb–0.75Si in the condition after LHT at 750 °C for 10 min (*a*), after annealing at 850 °C for 1 h (*b*)

**Table 2.** Mechanical properties of EB welded joints of heat-resistant titanium pseudo-α-alloy Ti–6.5Al–5.3Zr–2.2Sn–0.6Mo–0.5Nb–0.75Si, in as-welded condition

| Mode | $T_{pr}$, °C | $T_{LHT}$, °C | $\sigma_t$, MPa | $\sigma_{0.2}$, MPa | $\delta_s$, % | *KCV*, J/cm$^2$ |
|---|---|---|---|---|---|---|
| As-annealed base metal | – | – | 1027 | 996 | 2.7 | 13.9 |
| EBW, mode 1 | – | – | 996 | 901 | – | 12.3 |
| EBW with preheating, mode 2 | 400 | – | 910 | 840 | – | 17.9 |
| EBW with LHT, mode 3 | –»– | 750 | 1041 | 1012 | – | 17.4 |

with LHT suggested that microhardness distribution in different areas of the welded joint is still nonuniform (Figure 14, *a*). Note that the proposed LHT widened the welded joint HAZ. The width of base metal area, where an increase in microhardness values to 3000 MPa occurred, expanded to that of the LHT zone, in this case to 30 mm. Furnace annealing should be used to achieve a completely homogeneous metal of the weld, HAZ and base metal. So, vacuum annealing of the welded joints at the temperature of 850 °C intensified the diffusion processes, which resulted in alloying element redistribution in the welded joint structure. Microhardness distribution in EB welded joint of heat-resistant titanium alloy Ti–6.5Al–5.3Zr–2.2Sn–0.6Mo–0.5Nb–0.75Si in as-annealed condition showed that the microhardness level in different areas of the welded joints is homogeneous, being at the level of base metal microhardness of 2100–2300 MPa.

Determination of mechanical properties of EB welded joint of heat-resistant titanium pseudo-α-alloy Ti–6.5Al–5.3Zr–2.2Sn–0.6Mo–0.5Nb–0.75Si led to the conclusion that the lowest strength values in as-welded condition are demonstrated by joints made by EBW with preheating to 400 °C, and they are equal to 910 MPa (Table 2) or 88 % of BM strength after annealing. The strength values are the highest in welded joints produced by EBW with LHT at 750 °C (mode 3, see Table 1) and they are equal to 1041 MPa, which is at the level of BM strength. Welded joints made by simple EBW without application of additional technological measures, have medium values of strength at the level of 996 MPa or 97 % of BM strength.

The main difference of welded joints of heat-resistant titanium pseudo-α-alloy Ti–6.5Al–5.3Zr–2.2Sn–0.6Mo–0.5Nb–0.75Si is the fact that application of just the preheating leads to coarsening of the welded joint microstructure and deterioration of their mechanical properties, while for pseudo-β-alloys EBW in combination with preheating allows producing a finer microstructure of the welded joints, increasing the welded joints strength and ensuring equal strength of the welded joints to base metal [24].

Thus, EBW application in combination with LHT when producing welded joints of heat-resistant titanium pseudo-α-alloy Ti–6.5Al–5.3Zr–2.2Sn–0.6Mo–0.5Nb–0.75Si allows making welded joints equal in strength to the base metal, and additional furnace annealing should be used to ensure a homogeneous structure in all the zones of the welded joint, including the HAZ.

## CONCLUSIONS

1. Investigations of the structure of welded joints of heat-resistant titanium alloy Ti–6.5Al–5.3Zr–2.2Sn–0.6Mo–0.5Nb–0.75Si revealed that application of EBW with LHT at 750 °C leads to reduction of the size of packages with Widmanstatten morphology from 50–100 to 20–50 μm and increase in welded joint strength from 996 to 1041 MPa.

2. EBW of heat-resistant Ti–6.5Al–5.3Zr–2.2Sn–0.6Mo–0.5Nb–0.75Si alloy with application of just the preheating leads to a significant coarsening of the weld structure and to occurrence of the grain growth processes in the HAZ with larger packages of Widmanstatten morphology of 50–100 μm size forming in the metal, which is greater than in the base metal structure, and to deterioration of the welded joint mechanical structure.

3. Determination of the mechanical properties of the welded joints of heat-resistant titanium pseudo-α-alloy Ti–6.5Al–5.3Zr–2.2Sn–0.6Mo–0.5Nb–0.75Si produced by EBW with application of additional technological measures, such as preheating and local heat treatment, suggests that welded joints made by EBW with LHT at 750 °C have the greatest strength values, equal to 1041 MPa, which is at the level of base metal strength.

4. A technological process of EBW of heat-resistant titanium pseudo-α-alloy Ti–6.5Al–5.3Zr–2.2Sn–0.6Mo–0.5Nb–0.75Si with LHT is proposed, which envisages preheating of the welded joints to the temperature of 400 °C and LHT at 750 °C, which ensures formation of a highly homogeneous fine microstructure in welded joints and provides strength values of the joints of 1041 MPa in as-welded condition, which is at the level of base metal strength.

## REFERENCES

1. (2003) *Titanium and titanium alloys. Fundamentals and applications*. Ed. by Leyens and M. Peters. Weinheim, WILEY-VCH Verlag GmbH & Co, KGaA.

2. Ertuan Zhao, Shichen Sun, Yu Zhang (2021) Recent advances in silicon containing high temperature titanium alloys. *J. of Materials Research and Technology*, **14**, September–October, 3029–3042.
3. Firstov, S., Kulak, L., Miracle, D. et al. (2001) *Proc. of 8th Annual Inter. Conf. on Composites Engineering ICCE/8, Aug. 5–11, Tenerife, Canary Islands, Spain*. Ed. by D. Hui, 245–246.
4. Saha, R.L., Nandy, T.K., Misra, R.D.K. (1991) Microstructural changes induced by ternary additions in a hypo-eutectic titanium-silicon alloy. *J. of Materials Sci.*, **26**, 2637–2644.
5. Firstov, S.O., Kulak.L.D., Kuzmenko, M.M., Shevchenko, O.M. (2018) Alloys of Ti–Al–Zr–Si system for high temperature operation. *Fiz.-Khimich. Mekhanika Materialiv,* 54(**6**), 30–35 [in Ukrainian].
6. Shichen Sun, Hongze Fang, Yili Li et al. (2023) Formation mechanism and effect on the mechanical properties of TiSi phase for Ti–5Al–5Mo–5Cr–3Nb–2Zr alloyed by silicon. *J. of Alloys and Compounds*, 938(**25**), 168510.
7. Hong Feng, Shuzhi Zhang, Fan Peng et al. (2023) Enhanced mechanical properties of a near-α titanium alloy by tailoring the silicide precipitation behavior through severe plastic deformation. *Materials Sci. and Eng*., 880(**26**), 145356.
8. Wu, T., Beaven, P., Wagner, R. (1990) The $Ti_3$ (Al, Si) + $Ti_5$ $(Si, Al)_3$ eutectic reaction in the Ti–Al–Si System. *Scripta Metallurgica*, **24**, 207–212.
9. Bulanova, M., Tretyachenko, L., Golovkova M. (1997) Phase equilibria in the Ti-rich corner of the Ti–SiAl system. *Zeitschrift Metallkunde*, **88**, 257–265.
10. Mazur, V.I., Taran, Y.N., Kapustnikova, S.V. et al. (1994) *Titanium matrix composites*. US Pat. No. 5366570, Nov. 22.
11. Hayat, M.D., Singh, H., He, Z., Cao, P. (2019) Titanium metal matrix composites: An overview. Pt A. *Composites*, 121418–121438. DOI: https://doi.org/10.1016/j.compositesa.2019.04.005
12. Akhonin, S.V., Vrzhizhevsky, E.L., Belous, V.Yu., Petrichenko, I.K. (2017) Influence of preheating parameters and local heat treatment on structure and properties of dispersion-strengthened joints of silicon-containing titanium alloys made by electron beam welding. *The Paton Welding J*., **7**, 43–47. DOI: https://doi.org/10.15407/tpwj2017.07.09
13. Li, Y., Wang, H., Han, K. et al. (2017) Microstructure of Ti–45Al–8.5Nb–0.2W–0.03Y electron beam welding joints. *J. of Materials Proc. Technology*, **250**, 401–409.
14. Kurashkin, S.O., Tynchenko, V.S., Seregin, Y.N. et al. (2020) The model of energy distribution during electron beam input in welding process. *J. of Physics: Conf. Series*, 1679(**4**), 042036. IOP Publishing.
15. Seregin, Y.N., Murygin, A.V., Laptenok, V.D., Tynchenko, V.S. (2018) Modeling of electron beam distribution in electron beam welding. *IOP Conf. Series: Materials Sci. and Eng*., 450(**3**), 032036. IOP Publishing.
16. Liu, P., Zhang, G.M., Zhai, T., Feng, K.Y. (2017) Effect of treatment in weld surface on fatigue and fracture behavior of titanium alloys welded joints by vacuum electron beam welding. *Vacuum*, **141**, 176–180.
17. Schmidt, P. (2019) Vorteile und Besonderheiten: Elektronen Strahlschweißen von Titanbauteilen. *Der Praktiker*, **4**, 158–162.
18. Zhao, X., Lu, X., Wang, K., He, F. (2022) Investigation on the microstructure and mechanical properties of Ti6Al4V titanium alloy electron beam welding joint. In: Proc. of the Institution of Mechanical Eng., Pt C. *J. of Mechanical Eng. Sci*., 236(**6**), 2957–2966.
19. Hansen, M., Kessler, H.D., McPherson, D.J. (1952) *Transact. Amer. Soc. Met*., **44**, 518.
20. Akhonin, S., Hryhorenko, G., Berdnikova, O. et al. (2019) Fine structure of heat-resistant titanium alloys welded joints. In: *Proc. of 9th Inter. Conf. on Nanomaterials: Applications & Properties (NAP-2019). September 15–20, Odessa, Ukraine*. Pt 1., Sumy, Sumy State University, 1–5.
21. Pederson, R., Niklasson, F., Skystedt, F., Warren, R. (2012) Microstructure and mechanical properties of friction- and electron-beam welded Ti–6Al–4V and Ti–6Al–2Sn–4Zr–6Mo. *Materials Sci. and Eng., A*, **552**, 555–565.
22. Akhonin, S.V., Berezos, V.O., Pikulin, O.M. et al. (2022) Producing high-temperature titanium alloys of Ti–Al–Zr–Si–Mo–Nb–Sn system by electron beam melting. *Suchasna Elektrometal*., **2**, 3–9. DOI: http://doi.org/10.37434/sem2022.02.01
23. Akhonin, S.V., Severin, A.Yu., Pikulin, O.M. et al. (2022) Structure and mechanical properties of high-temperature titanium alloy of Ti–Al–Zr–Si–Mo–Nb–Sn system after deformation treatment. *Suchasna Elektrometal*., **4**, 43–48. DOI: http://doi.org/10.37434/sem2022.04.07
24. Akhonin, S.V., Belous, V.Yu., Selin, R.V. et al. (2018) Electron beam welding and heat treatment of welded joints of high-strength pseudo-β titanium alloy VT19. *The Paton Welding J*., **7**, 10–14. DOI: http://dx.doi.org/10.15407/tpwj2018.07.02

## ORCID

S.V. Akhonin: 0000-0002-7746-2946,
V.Yu. Bilous: 0000-0002-0082-8030,
E.L. Vrzhyzhevskyi,: 0000-0001-8651-8510,
R.V. Selin: 0000-0002-2990-1131,
I.K. Petrychenko: 0009-0008-1097-7137,
S.L. Schwab: 0000-0002-4627-9786

## CONFLICT OF INTEREST

The Authors declare no conflict of interest

## CORRESPONDING AUTHOR

V.Yu. Bilous
E.O. Paton Electric Welding Institute of the NASU
11 Kazymyr Malevych Str., 03150, Kyiv, Ukraine.
E-mail: belousvy@gmail.com

## SUGGESTED CITATION

S.V. Akhonin, V.Yu. Bilous, E.L. Vrzhyzhevskyi, R.V. Selin, I.K. Petrychenko, S.L. Schwab, S.L. Antonyuk (2025) Structure and properties of welded joints of heat-resistant titanium alloy of Ti–Al–Zr–Sn–Mo–Nb–Si system produced by electron beam welding. *The Paton Welding J*., **2**, 13–23.
DOI: https://doi.org/10.37434/tpwj2025.02.03

## JOURNAL HOME PAGE

https://patonpublishinghouse.com/eng/journals/tpwj

Received: 11.10.2024
Received in revised form: 25.11.2024
Accepted: 31.03.2025